Grandcanonical simulations of solvated ideal fermions. Evidence for phase separation

A. Alavi and D. Frenkel

Citation: The Journal of Chemical Physics **97**, 9249 (1992); doi: 10.1063/1.463300
View online: http://dx.doi.org/10.1063/1.463300
View Table of Contents: http://scitation.aip.org/content/aip/journal/jcp/97/12?ver=pdfcov
Published by the AIP Publishing

Grand-canonical simulations of solvated ideal fermions. Evidence for phase separation

A. Alavi and D. Frenkel
FOM Instituut voor Atoom-en Molecuulfysica, Kruislaan 407, 1098 SJ Amsterdam, The Netherlands

(Received 7 May 1992; accepted 10 September 1992)

A novel scheme to perform finite-temperature grand-canonical simulations of ideal fermions in arbitrary external potentials is introduced. This scheme is based on the evaluation of the grand-canonical function of lattice fermions. As an application, we present results on the phase behavior of a mixture of fermions and hard spheres. A simple analytic model of solvated fermions in a hard-sphere fluid is also studied. We address here the possibility of phase separation between a pure delocalized phase of fermions and a homogeneous solution of solvated fermions. These calculations indicate that the homogeneous phase is expected to be stable only at low fermion concentration and low thermal wavelengths. The fermion simulations indicate that such phase separation is a likely scenario.

I. INTRODUCTION

In the study of the equilibrium properties of a quantum particle in an arbitrary external potential, one central object of calculation is the equilibrium density matrix $\rho(\mathbf{r},\mathbf{r}';\beta)$. The importance of this matrix stems from the fact that the partition function Z of the system, and the equilibrium expectation values of operators $\langle A\rangle$, can be expressed in terms of it:

$$Z=\mathrm{Tr}(\rho), \tag{1}$$

$$\langle A\rangle=\mathrm{Tr}(A\rho)/Z. \tag{2}$$

In the path-integral formulation of quantum mechanics, this density matrix is expressed in terms of a Feynman path integral,[1] as the sum of the exponentially weighted imaginary-time action functionals of all paths $\mathbf{r}(u)$ starting at $u=0$ at $\mathbf{r}$ and ending at $u=\beta\hbar$ at $\mathbf{r}'$:

$$\rho(\mathbf{r},\mathbf{r}';\beta)=\int_{\mathbf{r}}^{\mathbf{r}'}\mathscr{D}\mathbf{r}(u)\exp\left(-\hbar^{-1}\int_0^{\beta\hbar}du H[\mathbf{r}]\right). \tag{3}$$

$H[\mathbf{r}(u)]$ is the Hamiltonian for the path $\mathbf{r}(u)$:

$$H=\tfrac{1}{2}m\dot{\mathbf{r}}^2+V[\mathbf{r}]. \tag{4}$$

m is the particle mass and $\beta=1/k_BT$ is the inverse temperature. Of course the actual calculation of such path integrals, as expressed in Eq. (3), is a formidably difficult task for all but the simplest potentials V. In order to make progress, some approximations need to be introduced. One such approximation is based on the "ring–polymer" analogy. In this approach[2] the continuous path $\mathbf{r}(u)$ is discretized into P "beads," so that the action integral of Eq. (4) is approximated as a sum:[3]

$$\frac{1}{\hbar}\int_0^{\hbar\beta}du\left(\frac{1}{2}m\dot{\mathbf{r}}^2+V[\mathbf{r}]\right)\approx\sum_i^P\frac{P}{2\lambda_B^2}(\mathbf{r}_i-\mathbf{r}_{i+1})^2+\frac{\beta V(\mathbf{r}_i)}{P}, \tag{5}$$

where the square of the thermal de Broglie wavelength $\lambda_B^2=\hbar^2\beta/m$ has been introduced into the right-hand side of Eq. (5). $\mathbf{r}_i$ is the position of the ith bead. Since, for the calculation of the partition function and therefore the thermodynamic properties, what is required is information concerning only the diagonal elements $\rho(\mathbf{r},\mathbf{r},\beta)$ of the density matrix, it is necessary to impose the condition $\mathbf{r}_{P+1}=\mathbf{r}_1$: in other words that the string of beads is closed. The right-hand side of Eq. (5) is formally equivalent to the Hamiltonian of a flexible (non-self-avoiding) P-bead ring polymer in which neighboring beads interact with a harmonic potential of spring constant $P/\beta\lambda_B^2$ and whose interaction with the external potential is given by $V(\mathbf{r}_i)/P$. Therefore, the equilibrium properties of the electronic system are approximately equal to that of such a P bead ring polymer, the equivalence becoming exact in the limit $P\to\infty$. Since the equilibrium properties of the ring–polymer system can be obtained numerically using Monte Carlo or molecular-dynamics simulations, it follows that these latter methods provide a route to the equilibrium properties of the electron. The need for the explicit calculation of the density matrix and partition function itself is thus circumvented.

On the other hand, knowledge of this partition function is often desirable for the calculation of certain thermal properties such as the excess chemical potential of the quantum particle.[4] In addition, as we shall show below, its calculation provides a convenient starting point for the calculation of partition functions of noninteracting many-fermion systems, *in which the sign problem is solved exactly*. One purpose of the present study is to point out that, under two controlled approximations, such partition functions can indeed be computed. Of course, noninteracting fermion problems can be solved in many other ways: direct diagonalization of the one-electron Hamiltonian being one obvious method. Our aim here is different. We wish to understand how the sign problem can be solved for this simple problem using path-integral ideas, since even this is by no means obvious. Sections II and III are devoted to this problem. In Sec. IV we briefly outline an efficient simulation technique to perform importance-sampling Monte Carlo calculations for quantum systems in the presence of *annealed* disorder, which is relevant to systems such as

solvated electrons in fluid environments. In Sec. V, we consider the application of our present scheme to a mixture of "classical" hard spheres and fermions. In that case our grand-canonical path-integral approach allows us to study the structure and phase behavior of a nontrivial model system.

Solvated electrons have been the subject of a number of recent numerical studies.[5–8] Much of the emphasis in these latter works has been on realistic models in the regime of very low electron density. For example, Deng, Martyna, and Klein studied bipolarons in metal–ammonia solutions. Study of higher electron concentrations has been hampered to a large extent by Fermion sign problems. The techniques presented in the present paper might therefore be useful in studying these more realistic systems at higher electron densities, for example, in the liquid-metal regime. The emphasis of the present paper, however, is not on realistic models. Finally, we should mention that our long-term goal is to study interacting fermion systems. Although some of the methods we discuss can be generalized to the interacting problem, their implementation requires algorithms with the same computational complexity of existing exact diaganolization methods. Solutions to the interacting problem, therefore, remain elusive. On this latter point, however, we should mention recent notable progress.[9–11]

II. CANONICAL AND GRAND-CANONICAL FUNCTIONS

Consider a cubic periodic box of volume L^3, and impose a grid of lattice spacing δ on this box, so that there are $N=(L/\delta)^3$ grid points in the box. Let the amplitude of being at site i and propagating in one "time step" to site j be ρ_{ij}. This amplitude, by analogy to the previous discussion, is given by[12]

$$\rho_{ij}=Ae^{-Pr_{ij}^2/2\lambda_B^2-\beta(V_i+V_j)/2P}, \tag{6}$$

where r_{ij} is the distance between the sites i and j, and V_i and V_j is the potential energy at sites i and j, respectively. A is a normalization constant, determined by the condition that the total amplitude for propagation of a free particle in one time step is unity:

$$\sum_j \rho_{ij}^{(0)}=1, \tag{7}$$

where $\rho^{(0)}$ is the free-particle propagator. What we require is the total amplitude $\rho_{ij}^{(P)}$ of propagating from site i to site j in P steps. Note that this quantity can be computed iteratively:

$$\rho_{ij}^{(P)}=\sum_k \rho_{ik}^{(P-1)}\rho_{kj}, \tag{8}$$

which expresses the fact that the total amplitude to get from i to j in P steps is equal to the sum over the amplitudes to get from i to k in $P-1$ steps times the amplitude from k to j in one step. In matrix form Eq. (8) can be expressed as

$$\rho^{(P)}=\rho^{(P-1)}\rho=\rho^P. \tag{9}$$

P, the number of steps to be propagated, depends on the thermal de Broglie wavelength of the particle (and hence the temperature) as well as on the lattice spacing δ. Its value can be calculated from the fact that the mean-square displacement of a particle that has propagated one time step should be be equal to λ_B^2/P. Thus, in three dimensions:

$$\frac{\sum_{j=1}^N r_j^2 e^{-Pr_j^2/2\lambda_B^2}}{\sum_{j=1}^N e^{-Pr_j^2/2\lambda_B^2}}=3\lambda_B^2/P. \tag{10}$$

r_j is the distance of j from the origin, and its square can be expressed as an integer multiple of δ $r_j^2=n_j\delta^2$. This enables us to express P as

$$P=x\lambda_B^2/\delta^2, \tag{11}$$

where x is a numerical constant determined by the solution to the equation:

$$\frac{\sum_{j=1}^N n_j e^{-n_j x/2}}{\sum_{j=1}^N e^{-n_j x/2}}=\frac{3}{x}. \tag{12}$$

For nearest-neighbor hopping on a cubic lattice, $x=3.432\ 217\ 8\ldots$. P is thus expressed as a simple function of β through Eq. (11). In what follows, a P dependence of any quantity implies the dependence of that quantity on β and δ through Eq. (11). Typically, for a given λ_B, we choose δ such that P is at least several hundred.

In general, we only require the partition function $Z(P)$, which is the trace of $\rho^{(P)}$. Since the trace of a symmetric matrix is invariant to its representation, Z can be expressed as follows:

$$Z(P)=\sum_i \rho_{ii}^{(P)}=\sum_i \lambda_i^P, \tag{13}$$

where the $\{\lambda_i\}$ is the set of eigenvalues of ρ.

This expression for the partition function of a single particle provides a convenient framework to discuss a *many*-fermion system as well. The key additional ingredient required when considering a many-fermion system is the condition that the elements of the density matrix be antisymmetric under odd permutations of fermionic paths. This requirement is the source of a fundamental difficulty in evaluating the partition function of a many-fermion system, namely that the weights of such exchanged paths need to be *subtracted* from the partition function. In general, these negative contributions almost cancel the positive contributions, leaving a relatively small (positive) number which is usually within the noise of the calculation. What is required is a method which yields this difference *directly*, without recourse to the numerically unstable procedure of calculating the positive and negative contributions separately and then performing the subtraction. The present approach can be used to do precisely this in the case for which the fermions are noninteracting. A two-fermion system serves to illustrate this assertion. The partition function for such a system, $Z(2,P)$, can be written as

$$Z(2,P)=\sum_{ij} \rho_{ii}^{(P)}\rho_{jj}^{(P)}-\rho_{ij}^{(P)}\rho_{ji}^{(P)}, \tag{14}$$

where the first term in Eq. (14) is the amplitude for a particle at i returning to i after P steps given that an particle at j returns to j after P steps, and the second (negative) term is the amplitude for i propagating to j in P steps and j propagating to i in the same time. This is the exchange term. Since the particles are independent, the sums over i and j can be done separately, yielding

$$Z(2,P)=Z(1,P)^2-Z(1,2P). \tag{15}$$

In the eigenvalue representation, Eq. (15) becomes expressible in a form in which the subtraction can be done *exactly*:

$$Z(2,P)=\left(\sum_i \lambda_i^P\right)^2-\sum_i \lambda_i^{2P}=\sum_{i\neq j}(\lambda_i\lambda_j)^P. \tag{16}$$

Since P can always be chosen to be even, the partition function is thus expressed as a sum of *positive* terms. This sum is asymptotically dominated by the two largest eigenvalues λ_1, λ_2 of ρ in the limit $\lambda_B^2 \sim P \to \infty$,

$$\lim_{\lambda_B\to\infty} Z(2,P)\sim(\lambda_1\lambda_2)^P. \tag{17}$$

Thus in this approach it is an *easier* task to compute low-temperature (rather than high-temperature) partition functions, a feature which is quite the reverse of standard path-integral procedures in which sign problems typically prevent the calculation of low-temperature properties.

It is a simple but tedious task to generalize Eq. (16) to an N-independent-fermion system. The partition function for this system is

$$Z(N,P)=\sum_{i\neq j\neq k\ldots}(\lambda_i\lambda_j\lambda_k\ldots)^P. \tag{18}$$

Notice that Eq. (18) contains a statement of the Pauli exclusion principle, namely that no state λ_i may be more than singly occupied (neglecting spin).

The discussion so far has concentrated on the evaluation of the N-independent particle partition function. However, it is often more natural when dealing with fermionic systems to work in an ensemble in which the chemical potential (which is closely allied to the Fermi level) is fixed. To work in this ensemble requires the calculation of the grand-canonical partition function. The above framework provides a remarkably simple route to this partition function as well. The fermion grand-canonical partition function $\Xi(\mu,\beta)$ is given by

$$\Xi(\mu,\beta)=\det(e^{\beta\mu}\rho^{(P)}+I). \tag{19}$$

To verify Eq. (19), we use the matrix identity $\det(A)=e^{\mathrm{Tr}[\log(A)]}$ to reexpress the determinant in terms of $\{\lambda_i\}$:

$$\det(e^{\beta\mu}\rho^{(P)}+I)=\prod_{i=1}^{N}(1+e^{\beta\mu}\lambda_i^P) \tag{20}$$

$$=\sum_{M=0}^{N} e^{M\beta\mu}\left[\sum_{i\neq j\neq k\ldots}(\lambda_i\lambda_j\lambda_k\ldots)^P\right] \tag{21}$$

$$=\sum_{M=0}^{N} e^{M\beta\mu}Z(M,P) \tag{22}$$

$$=\Xi(\mu,\beta). \tag{23}$$

The average number $\langle N_f\rangle$ of fermions in the system with chemical potential μ is given by $\beta\langle N_f\rangle=\partial\log\Xi/\partial\mu$, yielding

$$\langle N_f\rangle=\sum_i \frac{1}{1+e^{-\beta\mu}\lambda_i^{-P}}. \tag{24}$$

The occupation number n_i of state i is given by $1/(1+e^{-\beta\mu}\lambda_i^{-P})$, which is precisely the Fermi–Dirac distribution. Note that so far we have not considered spin. However, spin can be included straightforwardly: for spin-1/2 fermions, the appropriate grand-canonical function is simply the square of the determinant (19).

To make progress with numerical work, however, a second approximation is required since the calculation of the eigenvalues of ρ as it stands in Eq. (6) is difficult. As can seen from Eq. (6), the elements of the density matrix that describes short-time propagation between two sites decrease rapidly with the separation of these sites. We therefore assume that the short-time density matrix only connects a finite number of neighboring sites. Such an approximation renders ρ a sparse matrix, whose largest eigenvalues can be computed by standard techniques without difficulty. On a cubic lattice with N sites, ρ with nearest-neighbour hopping only, is an $N\times N$ matrix but has at most only $7N$ nonzero elements. $\rho^{(P)}$, on the other hand, is a dense matrix for all moderately large P: not only is the calculation of the eigenvalues of such matrices difficult (in fact, it is equivalent to diagonalizing the Hamiltonian), but also its storage requires N^2 words: on present-day supercomputers the largest full matrix which can be conveniently stored is $N\approx 5000$. In contrast, manageable grid sizes for storing ρ is well over a million lattice points. Notice that the short-time approximation can be relaxed in a controlled way, at the expense of computer time and storage, by allowing for successively longer short-time propagations. Note, in addition, that the *structure* of the lattice is unimportant in the calculation: we work with a cubic lattice for simplicity, but we could have chosen the N points on which to represent ρ in other ways as well.

III. FREE FERMIONS

It is instructive to see how the eigenvalues of ρ are related to that of the Hamiltonian H in a simple case where analytic calculations are feasible, for example, free fermions in a periodic box of length L. The eigenvalues of H for this system are

$$\epsilon_{\mathbf{k}}=\frac{\hbar^2k^2}{2m}, \quad k_x=2\pi n_x/L,... \tag{25}$$

and the Boltzmann weight for the kth state is

$$w_{\mathbf{k}}=\exp(-\beta\epsilon_{\mathbf{k}})=\exp(-\beta\hbar^2k^2/2m). \tag{26}$$

If we now consider a ρ on a cubic lattice with nearest-neighbor hopping only, and in addition for simplicty set $\rho_{ii}=0$, we obtain a band-diagonal matrix:

$$\rho_{ij}=\tfrac{1}{6}, \quad (i,j) \text{ nearest neighbors} \tag{27}$$

$$=0 \quad \text{otherwise.} \tag{28}$$

The eigenvalues for such a ρ are

$$\lambda_{\mathbf{k}}=\tfrac{1}{3}[\cos(k_x)+\cos(k_y)+\cos(k_z)],$$

$$k_x=2\pi n_x\delta/L.... \tag{29}$$

Expanding (29), we obtain

$$\lambda_{\mathbf{k}}=1-\tfrac{1}{6}k^2\delta^2+\mathcal{O}(k^4\delta^4) \tag{30}$$

$$=\exp(-k^2\delta^2/6)+\mathcal{O}(k^4\delta^4). \tag{31}$$

Upon taking the $P=3\beta\hbar^2/m\delta^2$ power of $\lambda_{\mathbf{k}}$ we obtain

$$\lambda_{\mathbf{k}}^P=\exp(-\beta\hbar^2k^2/2m)+\mathcal{O}(k^4\delta^4), \tag{32}$$

which to order $\mathcal{O}(k^4\delta^4)$ agrees with Eq. (26). The present approach, therefore, is valid only when the typical wave vectors of the occupied states are much smaller than $1/\delta$. Clearly the approach becomes exact when $\delta\to 0$.

IV. SAMPLING FLUID CONFIGURATIONS

Thus far, the discussion has been concerned with the evaluation of Z or Ξ for a fixed, static external potential. However, we are more often interested in situations in which this potential is not fixed, but changes under the influence of the fermions. Such is the case, for example, for an electron solvated in a classical *fluid*: here the potential posesses a great deal of disorder which can *anneal*. Under such circumstances, it is necessary to perform an ensemble average over different fluid configurations, weighted according to a probability density determined in part by the fermionic partition function. To this end, let the fluid consist of M particles, whose total (fluid–fluid) interaction energy is $V_F(\mathbf{r}^M)$. The partition function Z_T for the complete (fermion + fluid) system is

$$Z_T(M,\beta,\mu)=\int d\mathbf{r}^M e^{-\beta V_F(\mathbf{r}^M)}\Xi(\beta,\mu;\mathbf{r}^M). \tag{33}$$

In other words, the phase space of the fluid must be sampled with the relative probability density $e^{-\beta V_F}\Xi$. Importance-sampling Monte Carlo is one convenient way to achieve this.

It is important, however, that an efficient procedure exists to perform such sampling. For example, since the eigenvalue calculation is the costliest part of these calculations, it is desirable to know *before* such a calculation is undertaken the approximate change in the electronic partition function for a given (small) change in the fluid configuration. This change can be calculated using perturbation theory. Suppose the fluid configuration is changed randomly from $\mathbf{r}^M$ to $\mathbf{r}^M+\delta\mathbf{r}^M$. Denote the corresponding change in ρ by $\delta\rho$. What we seek are the changes in the spectrum of ρ. In first-order perturbation theory, the change to the kth eigenvalue is

$$\delta\lambda_k\approx v^{(k)}\delta\rho v^{(k)}, \tag{34}$$

where $v^{(k)}$ is the kth eigenvector of ρ. The corresponding changes δZ to the one-particle partition function and $\delta\Xi$ to the grand-canonical partition function are

$$\delta Z(P)\approx\sum_i P\lambda_i^{P-1}\delta\lambda_i, \tag{35}$$

$$\delta\Xi(\mu,P)\approx\Xi\sum_i Pn_i\delta\lambda_i/\lambda_i. \tag{36}$$

The idea is to *generate* configurations in a biased way, with the weight $W=Z+\delta Z$. In order to remove this bias, we *accept* such configurations according to the weight Z'/W, where Z' is the new, exact partition function: the division by W achieves the desired unbiasing. To perform such biased sampling, therefore, requires the additional calculation of some of the eigenvectors of ρ. For the one-particle partition function, calculation of the eigenvectors corresponding to the largest few eigenvalues suffices, whereas for the grand-canonical partition function, the eigenvectors corresponding to the occupied states ($n_i\approx 1$) are required. It is true that these additional calculations somewhat slow down the diagonalization part of the calculation. Yet they allow us construct a rather simple and efficient biased sampling technique.

V. AN APPLICATION: FERMIONS SOLVATED IN A HARD-SPHERE FLUID

As an application of the present scheme we have performed simulations of a mixture of ideal fermions and a hard-sphere fluid. This model might serve as a simple and crude realization of electrons solvated in a rare-gas fluid. A single electron dissolved in the hard-sphere fluid has been studied previously by Sprik, Klein, and Chandler,[13] using path-integral Monte Carlo techniques. In that work it was found that at a given thermal wavelength, and beyond a certain density of hard spheres, the electron would localize into a cavity, *devoid of solvent*. For example, at a thermal wavelength $\lambda_B=6\sigma$ (σ is the hard-sphere diameter), the electron cavity localized at a hard-sphere density of $\rho\sigma^3\approx 0.2$. Below this fluid density, the electron would appear delocalized over several fluid particles.

In the present work we consider the question of whether the localization of the electrons into solvent depleted regions could in turn lead to *phase separation* between regions which are hard sphere rich and regions which are fermion rich. Clearly, this question requires that Fermi–Dirac statistics be properly incorporated. The simulation scheme we outlined earlier therefore might be a good candidate to tackle this problem. First, however, we develop a simple model to describe this phase separation.

There are (at least) two distinct phases one might envisage in a hard-sphere fluid plus fermion mixture. One is

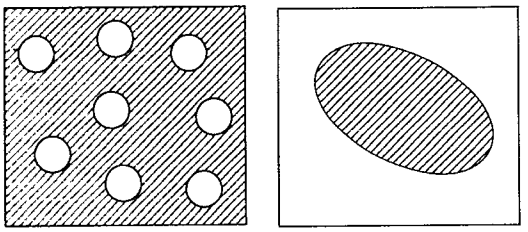

FIG. 1. Schematic representation of the cavity-rich phase of fermions in a homogeneous fluid (left), and a phase-separated, inhomogeneous, phase (right). In the latter picture, the fluid has formed a droplet and the fermions are delocalized.

a macroscopically homogeneous phase in which the fermions solvate into separate localized cavities, which in turn form a "solution" with the hard-sphere fluid. We shall call this homogeneous phase a "cavity-rich" phase. In the second phase, the system has phase separated into a hard-sphere rich region and a fermion rich region. Such a system would be macroscopically inhomogeneous, and in a finite periodic system would result in the formation of an interface (see Fig. 1). In this latter phase the fermions are delocalized and occupy a single macroscopic volume. As a result, Fermi–Dirac statstics plays an important role in determining the free energy of the fermions. Which of these two phases is stable is determined by their relative free energies. To estimate this below, we construct a simple model.

For the case of the homogeneous phase, consider a box of dimensions L^3 in which there are solvated N_f fermions in cavities of dimension $a^3 \ll L^3$. This a is as yet undetermined. The electronic states in these cavities will be particle-in-a-box-like, with a ground-state energy $\epsilon \sim 1/a^2$. A crude estimate for the fermionic energy will therefore be $\sim N_f/a^2$. To estimate the total free energy of the system we require the free energy of the fluid. To this end, we model the homogeneous phase as consisting of a binary mixture of hard spheres: the hard-sphere fluid itself, consisting of spheres of diameter $\sigma=1$, and the fermion cavities, which we view as hard spheres of as yet undetermined diameter a. The aim here is to employ the equation of state of a binary hard-sphere mixture proposed by Mansoori *et al.*[14] These authors have given an expression, based on the Carnahan–Starling equation of the pure hard-sphere fluid, for the excess free-energy of a binary hard-sphere mixture. This expression depends on three parameters: a/σ, the ratio of the hard-sphere diameters, the total number density $\rho=(N_a+N_f)/V$, and the mole fraction of one the components, say of the fluid, x_a. Denote this free energy as $F_M(x_a,\rho,a)$. Then the total free energy of the homogeneous phase is

$$\frac{\beta F_H}{N}=x_a \log(\rho x_a)+x_f \log(\rho x_f)+F_M(x_a,\rho,a) + \frac{\pi^2}{2}\left(\frac{\lambda_B}{a}\right)^2 x_f, \tag{37}$$

where $x_f=1-x_a$ is the fermion mole fraction. To compute the conditions for phase coexistence we work at constant pressure, which requires us to calculate Gibbs free energies. The homogeneous phase Gibbs energy is given by

$$G_H/N=F_H/N+P/\rho, \tag{38}$$

where ρ is implicitly determined by the Mansoori equation of state $\beta P/\rho=f(x_a,\rho,a)$.[14] G_H must be minimized with respect to a, at constant pressure, i.e.,

$$(\partial G_H/\partial a)_{x_a\lambda_B P}=0. \tag{39}$$

It is simple to show from the definitions of G, F, and P that

$$(\partial G/\partial a)_{x_a\lambda_B P}=(\partial F/\partial a)_{x_a\lambda_B \rho}. \tag{40}$$

Therefore to compute the minimum Gibbs energy (with respect to a) for a given βP, x_a, and λ_B we first solve the pair of equations:

$$(\partial F/\partial a)_{x_a\lambda_B \rho}=0, \tag{41}$$

$$\beta P/\rho=f(x_a,\rho,a) \tag{42}$$

subject to the constraint that the total packing fraction is less than unity:

$$\eta=\pi\rho(x_a+x_f a^3)\leqslant 1. \tag{43}$$

The solution to these equations then determines ρ, a, and F_H, from which we obtain G_H using Eq. (38).

At phase coexistence, we assume that a pure fermion phase coexists with a hard-sphere fluid in which there may be solvated a finite concentration of fermions: the chemical potential of the fermions should be equal in the two phases. This concentration can be calculated using a procedure analogous to the equal tangent construction used to compute the coexistence curve of demixed binary mixtures. Let $G_H(\beta P,\lambda_B,x_a)$ be the Gibbs energy of the homogeneous phase, as determined in the manner described in the preceding paragraph, and let $G_F(\beta P,\lambda_B)$ be the Gibbs energy of the pure fermion phase. The equality of fermion chemical potentials in the two phases implies the following equation:

$$G_F(\beta P,\lambda_B)=G_H(\beta P,\lambda_B,x_a)-x_a(\partial G_H/\partial x_a)_{\beta P,\lambda_B}, \tag{44}$$

the solution of which determines x_a, the mole fraction of hard spheres at coexistence in the cavity-rich, homogeneous, phase. For a given $\beta P,\lambda_B$, we solve this equation numerically. Finally, to obtain a phase diagram at constant pressure, we solve this equation for a variety of values of λ_B.

To complete the specification of this model, we need to give $G_F(\beta P,\lambda_B)$, the Gibbs energy of the pure fermion phase. Here we employ the low-temperature form for this Gibbs energy:[15]

$$\frac{\beta G_F}{N}=\frac{(30\pi^2\beta P\lambda_B^3)^{2/5}}{2}. \tag{45}$$

In Fig. 2(a), we show the resulting x_a, λ_B phase diagram, for $\beta P\sigma^3=0.31$ (at this pressure the density of the pure hard-sphere fluid is $\rho\sigma^3=0.2$). The cavity-rich phase is stable only in a relatively small region, at high fluid con-

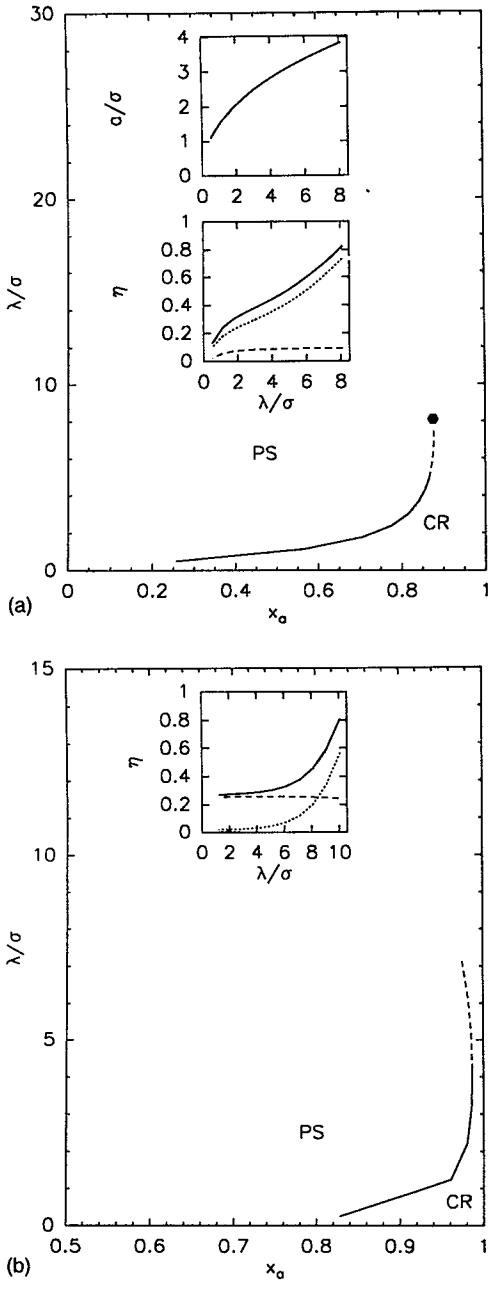

FIG. 2. (a) Phase diagram of the hard-sphere fluid and fermion mixture at $\beta P\sigma^3=0.31$. At this pressure, the density of a pure hard-sphere fluid is $\rho\sigma^3=0.2$. PS, phase-separated; CR, cavity-rich. The dot denotes the point beyond which the the phase-coexistence equation does not possess a valid solution. The upper inset shows the cavity size at phase coexistence. The lower inset shows the packing fractions: the solid line is the total packing fraction, the dotted line is the fermion component, and the dashed line is the hard-sphere component. (b) Same as (a), but at the pressure $\beta P\sigma^3=1.63$.

centrations and small thermal wavelengths (high temperatures). In the insets of the same figure, we show the cavity size and packing fractions at coexistence in the cavity-rich phase. The present model of the homogeneous phase cannot be expected to be reliable at high packing fractions where the Mansoori equation of state is also unreliable. Indeed, the coexistence curve changes in a surprisingly steep manner for $\lambda_B>6\sigma$, where packing fractions are large, and ends at $\lambda_B\approx 8\sigma$, where Eq. (44) ceases to have valid solutions. The lack of existence of valid solutions beyond some value of λ_B is associated with the requirement that the total packing fraction must be less than unity. Clearly, there are a number of ways of improving the present calculations: use of finite-temperature corrections to the Fermi gas Gibbs energy Eq. (45), and consideration of excited cavity states being obvious candidates. Nevertheless, the qualitative picture of phase separation is expected to hold with these refinements as well.

Phase separation in a mixture of ideal fermions and hard spheres should contain some of the physics of the phase separation which occurs in helium plus metal mixtures. An important and intriguing example of such phase separation is provided by the hydrogen–helium planet Saturn. The core of Saturn is thought to consist of nearly pure helium,[16] while at the relevant conditions ($T\approx 10^4$ K, $P\approx$1–10 Mbar) the hydrogen probably is metallic. If we view the helium as "hard spheres," and the metallic hydrogen as an independent electron gas (in which the hydrogen nuclei play the role of a neuturalizing background), we might expect on the basis of our calculations that such a mixture would phase separate. Calculation of phase diagrams at higher pressures [Fig. 2(b)] indicates that the homogeneous phase occupies an even smaller region of the x_a-λ_B plane, with phase separation being nearly complete at $\lambda_B=2\sigma$ (for $\sigma=3$ Å this λ implies a temperature of $T\approx 10^4$ K). Clearly, our model is a gross oversimplification of the real system. Nevertheless, since part of the driving force for phase separation in both cases is similar—the fermions undergoing a localization–delocalization transition—it is tempting to speculate that this same mechanism plays some role in the apparent demixing of hydrogen and helium in the interior of Saturn. We hope to address these questions in a more systematic way in a future publication.

VI. SIMULATIONS

We have performed grand-canonical simulations of fermions in a low-density hard-sphere fluid to test some of the above predictions. A periodic cubic simulation box of dimensions $L^3=(8\sigma)^3$ was considered, and grid sizes N in the range $16^3\leqslant N\leqslant 32^3$. Simulations were performed at the thermal wavelength $\lambda_B=3.8\sigma$, corresponding to ring lengths P determined from Eq. (11) of $191\leqslant P\leqslant 764$, and at a variety of hard-sphere densities $0.1\leqslant\rho\sigma^3\leqslant 0.35$, and electronic chemical potentials $\beta\mu\leqslant 20$ (corresponding to an average number of fermions $\langle N_f\rangle\leqslant 20$, depending, of course, on $\rho\sigma^3$ and $\beta\mu$). For a given hard-sphere configuration, up to the largest 30 or so eigenvalues and eigenvectors of the short-time propagator ρ were computed using Lanczos diagonalization.[17] Typical runs consisted of about 2000 Monte Carlo (MC) cycles of equilibration, and between 2000 and 5000 cycles for production, the acceptance ratios being about 90% at low μ and somewhat lower at high μ. Such a high acceptance ratio is a consequence of the staged sampling procedure we outlined earlier.

The grand-canonical partition function Ξ and average number of fermions $\langle N_F\rangle$ for a given hard-sphere config-

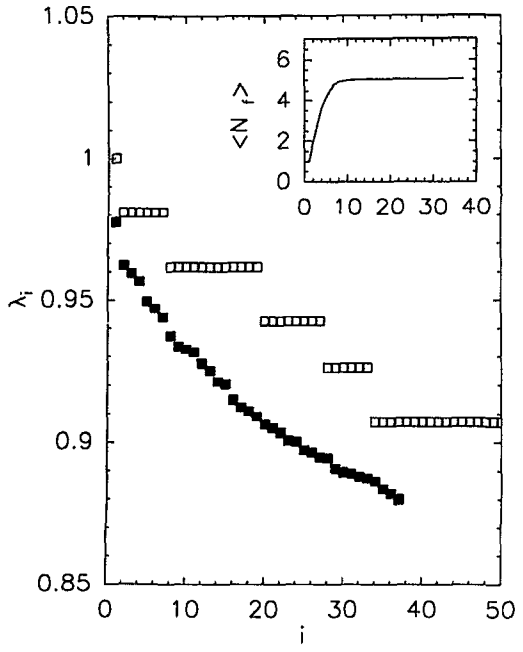

FIG. 3. An example of the first few eigenvalues of ρ for a typical, equilibrated configuration of hard spheres at $\rho\sigma^3=0.23$. The open squares represent the eignevalues of the free propagator. The inset shows the total number of fermions as a function of the eigenvalue index of this configuration.

uration were calculated using Eqs. (20) and (24), respectively, and the fluid configurations were sampled according to the relative probability density given by Eq. (33). As a reference calculation, we also performed a different set of simulations in which hard-sphere configurations were sampled without regard to the electronic partition function, namely with the relative probability density $P_0 = e^{-\beta V_F}$. The difference $\langle \cdots \rangle_\Xi - \langle \cdots \rangle_0$ in an ensemble average gives the (excess) contribution to that average due to the presence of fermions.

As an example of the eigenvalue structure of ρ in the presence of the hard-sphere fluid, we have plotted in Fig. 3 the first few eigenvalues of ρ, for a typical equilibrated configuration of hard spheres (at a density $\rho\sigma^3=0.23$). In this figure we also show the eigenvalues of ρ for the free-fermion problem. The interesting feature to note is the lifting of the degeneracies of the eigenvalues of the free-particle propagator by the external potential; in all cases the eigenvalues have been shifted downwards, an obvious consequence of the repulsive nature of the hard-sphere potential. In the same figure we also plot the total number of fermions as a function of i, the eigenvalue index, at a chemical potential $\mu=10k_BT$. It is clear that only the first ten states are substantially occupied. The calculation of the grand-canonical function, therefore, is complete after inclusion of these ten levels.

In Table I, we summarize the results for the equation of state of fermions in the hard-sphere fluid obtained, giving the equilibrium average number of fermions $\langle N_f \rangle$ as a function of $\beta\mu$ and $\rho\sigma^3$. The most extensive runs at different μ have been performed at the hard-sphere density $\rho\sigma^3$

TABLE I. Average fermion density as a function of $\rho\sigma^3$ and $\beta\mu$.

$\rho\sigma^3$	$\beta\mu$	$\langle N_F \rangle$
0.15	6	1.4
0.15	8	4.2
0.15	10	8.3
0.18	8	3.0
0.18	10	6.8
0.23	7	0.4
0.23	8	1.6
0.23	10	4.5
0.23	11	5.6
0.23	13	9.1
0.23	15	13.0
0.23	17	17.0
0.23	19	22.0
0.25	10	3.9
0.25	12	6.0
0.25	14	9.1
0.3	10	0.8
0.3	10	6.2
0.35	10	0.0
0.35	14	3.2

$=0.23$. In Fig. 4, we have plotted $\langle N_f \rangle$ and $\langle N_f \rangle_0$ against $\beta\mu$ at $\rho\sigma^3=0.23$. It is clear that at low values of $\beta\mu(<5)$, the fermionic density is negligibly small, while above this value the fermion density rises fairly sharply, and considerably more quickly than in the case where the sampling of the fluid is done irrespective of the fermionic partition function. The reason for this behavior is closely related to the structural changes which the fermions induce in the hard-sphere fluid. One crude way of studying such changes

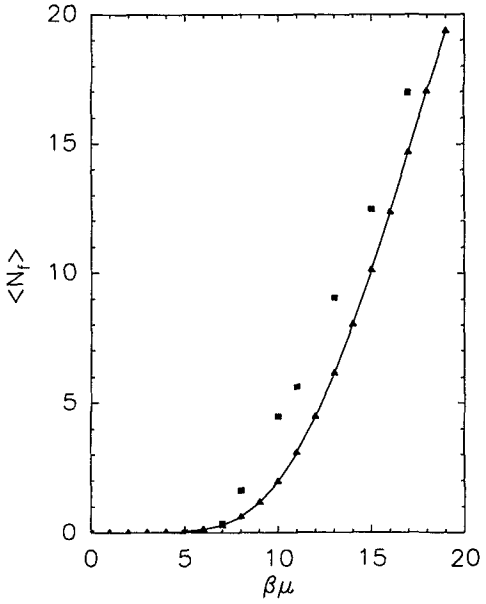

FIG. 4. The average total number of fermions $\langle N_f \rangle$. The squares denote the number of fermions in which the hard-sphere fluid has been sampled from the relative probability density $e^{-\beta V}\Xi$, whereas the triangles denote the number of fermions in which the hard-sphere fluid has been sampled on $e^{-\beta V}$. The excess number of fermions in the former case is clearly evident.

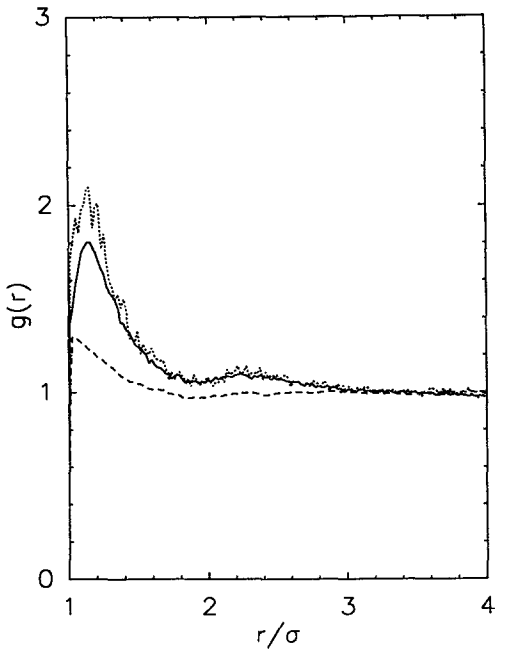

FIG. 5. Radial distribution functions $g(r)$ of the hard-sphere fluid. (a) $g(r)$ of the pure fluid at $\rho\sigma^3=0.23$. (b) $g(r)$ at $\beta\mu=10$. (c) $g(r)$ at $\beta\mu=15$.

is through the radial distribution function of the hard-sphere fluid. Examples of $g(r)$ are shown in Fig. 5: the hard-sphere fluid at $\rho\sigma^3=0.23$, and this same fluid with fermion chemical potential $\beta\mu=11$ and 15. It is clear that in the latter two cases, there is a large enhancement of the first peak of the radial distribution function, i.e., the fluid has clustered. Inspection of snapshots (e.g., Fig. 6) of the hard-sphere configuration confirm this general picture: large percolating voids have appeared. The system appears to be on the onset of phase separation. Since the present simulations are constant volume calculations, direct comparison with the phase diagram of the preceding section is not possible. Phase separation in the present case manifests itself through the clustering of the hard spheres into a liquidlike droplet, while the fermions propagate in the remaining volume. One consequence of phase separation is that the one-electron states *delocalize*. In a finite periodic system such delocalized states will be box quantized. For the present system size (a box of 8σ and $\lambda_B=3.8\sigma$, the spacing between the one-electron levels is of the order k_BT. We have not investigated the effect of the system size dependence on out results, though we would expect that phase separation would be driven more strongly for larger systems (the spacing drops as $1/L^2$, and therefore the consequent lowering of fermion kinetic energy upon delocalization is greater). However, this point remains to be investigated more thouroughly.

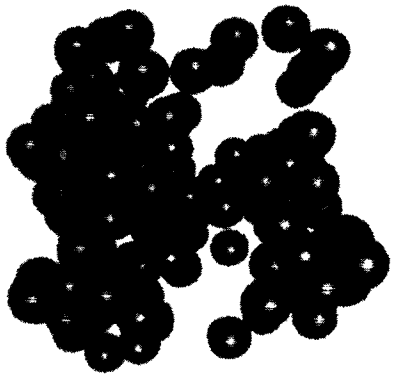

FIG. 6. Snapshot of an equilibrated hard sphere at $\rho\sigma^3=0.25$ and fermion $\beta\mu=14$.

One unusual, and almost certainly spurious, feature of the radial distribution functions should be noted, namely that the maximum of these functions is not at $r=\sigma$, but slightly higher values. This situation was found not to change by performing longer simulations, and is therefore apparantly not due to lack of equilibration. However, in simulations in which the fermions propagate on a finer lattice, it was found that this peak shifts to values of r closer to σ. This is some indication that for the present hard-sphere system convergence may not have been achieved. It is, in fact, not surprising that the present, rather coarse discretization of the one-particle propagator does not reproduce the properties of the fermions close to a hard, smooth surface. In fact, this problem is well known in path-integral MC simulations of quantum particles with hard-core interactions. In general, this problem can be resolved by using a better approximation for the high-temperature propagator (e.g., Barker's "image approximation." [18] However, such improved propagators are not easily included in the present discretised scheme.

Finally, we should add that phase separation in the present system is remarkable because our model contains *no explicit attractive interactions whatsoever*: the clustering of hard spheres is driven purely by repulsive interactions. There exists a closely related classical analogy, namely in the demixing of mixtures of ideal classical polymers and hard spheres.[19] In the latter system, the driving force for hard-sphere clustering is *purely* entropic: the number of random walks, and hence polymer entropy, is greatly increased by the clustering of hard spheres. However, the analogy should not be stretched. In the case of fermions, this intuitive picture is complicated not only by Fermi–Dirac statistics, whose effect is to introduce an effective replusion between fermions, but also by the ubiquitous, and highly nontrivial, contribution of kinetic energy to the free energy. The corresponding polymer kinetic energy makes a trivial contribution to the free energy.

VII. CONCLUSIONS

We have introduced a novel method to perform grand-canonical simulations of independent fermions in arbitrary external potentials. This scheme is based on the evaluation of the grand-canonical function of lattice fermions. Using this scheme, we have performed grand-canonical simulations of fermions in a hard-sphere fluid. In addition, we have studied a simple analytical model of ideal fermions solvated in a hard-sphere fluid. We address here the pos-

sibility of phase separation in a fermion hard-sphere fluid mixture, between a pure (delocalized) phase of fermions and a cavity-rich "solution" of fermions solvated in the hard-sphere fluid. The phase diagram for this model is numerically calculated. The homogeneous phase is expected to be stable only at low fermion concentrations and low thermal wavelengths. The fermion simulations indicate that such phase separation is a likely scenario.

ACKNOWLEDGMENTS

We thank D. Chandler, D. Lynden-Bell, R. M. Lynden-Bell, A. Lagendijk, and A. A. Louis for discussions. A. A thanks NATO/Science and Engineering Research Council for a fellowship, and the FOM-Institute for their hospitality. This work is part of the research program of FOM (Foundation for Fundamental Research on Matter), and is supported by The Netherlands Organisation for Scientific Research (NWO).

[1] R. P. Feynman and A. R. Hibbs, *Quantum Mechanics and Path Integrals* (McGraw-Hill New York, 1965).

[2] A large amount of literature exists on path-integral Monte Carlo techniques. For reviews see M. J. Gillan, in *Computer Modelling of Fluids, Polymers, and Solids*, edited by C. R. A. Catlow, S. C. Parker, and M. P. Allen, NATO ASI Series (Kluwer Academic, Dordrecht, 1990); D. Chandler, in *Liquids, Freezing and the Glass Transition*, edited by J. P. Hansen, D. Levesques, and J. Zinn-Justin, Les Houches Session LI, NATO ASI Series (North-Holland, Amsterdam, 1991). Other works of interest are L. D. Fosdick, J. Math. Phys. **3**, 1251 (1962); L. D. Fosdick and H. F. Jordan, Phys. Rev. **143**, 58 (1966); **171**, 128 (1968); J. Barker, J. Chem. Phys. **70**, 2914 (1979); D. Chandler and P. G. Wolynes, J. Chem. Phys. **74**, 7 (1981); M. Parrinello and A. Rahman, J. Chem. Phys. **80**, 860 (1984); D. Thirumalai, E. J. Brushkin, and B. J. Berne, J. Chem. Phys. **79**, 5063 (1983).

[3] One may take the view that Eq. (3) is in fact defined by the limit of $P \to \infty$ of Eq. (5).

[4] T. L. Beck, J. Chem. Phys. **96**, 7175 (1992).

[5] A. Selloni, R. Car, M. Parrinello, and P. Carnevali, J. Phys. Chem. **91**, 4947 (1987).

[6] Z. Deng, G. J. Martyna, and M. L. Klein, Phys. Rev. Lett. **68**, 2496 (1992).

[7] B. Space and D. F. Coker, J. Chem. Phys. **94**, 1976 (1991).

[8] B. Space and D. F. Coker, J. Chem. Phys. **96**, 652 (1992).

[9] D. M. Ceperley, Phys. Rev. Lett. **69**, 331 (1992).

[10] R. W. Hall and M. R. Prince, J. Chem. Phys. **95**, 5999 (1991).

[11] W. H. Newman and A. Kuki, J. Chem. Phys. **96**, 1409 (1992).

[12] This particular form of the propagator is called the primitive algorithm. Depending on the particular problem concerned, it may be advantageous to consider a different propagator. See G. Jacucci and E. Omerti, J. Chem. Phys. **79**, 3051 (1983).

[13] M. Sprik, M. L. Klein, and D. Chandler, J. Chem. Phys. **83**, 3042 (1985).

[14] G. A. Mansoori, N, F. Carnahan, K. E. Starling, and T. W. Leland, Jr., J. Chem. Phys. **54**, 1523 (1971).

[15] L. D. Landau and E. M. Lifshitz, *Statistical Physics*, 3rd ed. (Pergamon, New York, 1980).

[16] D. J. Stevenson and E. E. Salpeter, Astrophys. J. Suppl. Ser. **35**, 221 (1977).

[17] J. K. Cullum and R. A. Willoughby, *Lanczos Algorithms for Large Symmetric Eigenvalue Computations* (Birkhauser, Boston, 1985).

[18] J. Barker, J. Chem. Phys. **70**, 2914 (1979).

[19] E. J. Meijer and D. Frenkel, Phys. Rev. Lett. **67**, 1110 (1991).